

## **G $\beta$ interferes with Ca<sup>2+</sup>-dependent binding of synaptotagmin to the SNARE complex**

Eun-Ja Yoon, Tatyana Gerachshenko, Bryan D. Spiegelberg, Simon Alford, Heidi E. Hamm

Department of Pharmacology, Vanderbilt University Medical School, 23rd Ave. South at Pierce, Nashville, Tennessee, 37232 (E.J.Y., B.D.S., H.E.H.) and Department of Biological Sciences, University of Illinois at Chicago, 840 West Taylor, Chicago, Illinois, 60607 (T.G., S.A.).

**Running title:** G $\beta$  $\gamma$  mediated modulation of exocytosis.

**Address correspondence to:** Heidi E. Hamm, Department of Pharmacology, Vanderbilt

University Medical School, 23rd Ave. South at Pierce, Nashville, Tennessee, 37232, Phone:

(615) 343-3533; Fax: (615) 343-1084; E-mail: [heidi.hamm@vanderbilt.edu](mailto:heidi.hamm@vanderbilt.edu),

or Simon Alford, Department of Biological Sciences, University of Illinois at Chicago, 840 West

Taylor, Chicago, Illinois, 60607 Phone: (312)-355-0328; Fax: (312) 966-2805; E-mail:

[sta@uic.edu](mailto:sta@uic.edu)

**Number of text pages: 23**

**Number of figures: 8**

**Number of references: 40**

**Number of words in abstract: 235**

**Number of words in introduction: 605**

**Number of words in discussion: 784**

**Abbreviations:** SNARE; soluble N-ethylmaleimide-sensitive factor attachment protein receptor.

[Ca<sup>2+</sup>]; Ca<sup>2+</sup> concentration. SNAP25; Synaptosomal-associated protein of 25,000 dalton.

MIANS; 2-(4'-maleimidylanilino) naphthalene-6-sulfonic acid. BoNT/A; botulinum toxin A.

Synaptotagmin, Syt I (at figure); synaptotagmin I.

## Abstract

Presynaptic inhibitory GPCRs can decrease neurotransmission by inducing interaction of G $\beta\gamma$  with the soluble N-ethylmaleimide-sensitive factor attachment protein receptor (SNARE) complex. Previously, we showed that this action of G $\beta\gamma$  requires the carboxyl terminus of SNAP25 and is downstream of the well-known inhibition of Ca<sup>2+</sup> entry through voltage-gated calcium channels (VGCC). We proposed a mechanism in which G $\beta\gamma$  and synaptotagmin compete for binding to the SNARE complex. Here, we characterized the G $\beta\gamma$  interaction sites on syntaxin1A and SNAP25 and demonstrated an overlap of the G $\beta\gamma$ - and synaptotagmin I-binding regions on each member of the SNARE complex. Synaptotagmin competes in a Ca<sup>2+</sup>-sensitive manner with binding of G $\beta\gamma$  to SNAP25, syntaxin1A and the assembled SNARE complex. We predict based on these findings that at high intracellular Ca<sup>2+</sup> concentrations, Ca<sup>2+</sup>-synaptotagmin I can displace G $\beta\gamma$  binding, and the G $\beta\gamma$ -dependent inhibition of exocytosis can be blocked. We tested this hypothesis in giant synapses of the lamprey spinal cord, where 5-HT works via G $\beta\gamma$  to inhibit neurotransmission (Blackmer et al., 2001). We showed that increased presynaptic Ca<sup>2+</sup> suppresses the 5-HT- and G $\beta\gamma$ -dependent inhibition of exocytosis. We suggest that this effect may be due to Ca<sup>2+</sup>-dependent competition between G $\beta\gamma$  and synaptotagmin I for SNARE binding. This type of dynamic regulation may represent a novel mechanism for modifying transmitter release in a graded manner based on the history of action potentials that increase intracellular Ca<sup>2+</sup> concentrations and of inhibitory signals through Gi-coupled GPCRs.

## Introduction

Modification of neurotransmitter release by presynaptic G protein coupled receptors (GPCRs) is ubiquitous and vital to nervous system function.  $G\beta\gamma$  inhibits synchronous exocytosis directly at the SNARE complex, the heart of the fusion machinery (Blackmer et al., 2005; Blackmer et al., 2001; Chen et al., 2005; Gerachshenko et al., 2005; Man-Son-Hing et al., 1989; Silinsky, 1984; Takahashi et al., 2001), and consequently modifies the quantal size of release by causing transient fusion of vesicles in both lamprey giant synapses and mammalian chromaffin cells (Chen et al., 2005; Photowala et al., 2006). G proteins may also inhibit exocytosis through inhibition of VGCCs, blunting the influx of  $Ca^{2+}$  required for exocytosis (Herlitze et al., 1996; Ikeda, 1996).

Synaptotagmin I is thought to mediate the requirement for  $Ca^{2+}$  in the initiation of exocytosis. Prior to the fusion event, vesicles are primed by formation of a stable protein structure, the ternary SNARE complex, comprising the plasma membrane t-SNAREs, SNAP-25 and syntaxin, and the vesicular SNARE (v-SNARE), VAMP2 (Fig1A). Synaptotagmin, as the putative  $Ca^{2+}$  sensor, is thought to act as the trigger by which  $Ca^{2+}$  influx effects the fusion of primed vesicles (Bai et al., 2004; Maximov and Sudhof, 2005; Wang et al., 2006).

Given its central role in triggering exocytosis, interactions between synaptotagmins and the SNARE complex have been studied extensively. Upon  $Ca^{2+}$  binding to its C2 domains (Fig. 1A) during regulated exocytosis, synaptotagmin interacts with phospholipids and the SNARE complex (Perin et al., 1990; Schiavo et al., 1997). This interaction occurs through the H3 SNARE domain of syntaxin1A and the C-terminus of SNAP25 (Bai et al., 2004; Bennett et al., 1992; Chapman et al., 1995; Gerona et al., 2000). While the mechanism by which the SNARE complex initiates fusion is under debate (Rizo et al., 2006), interactions with synaptotagmin may

cause stabilized ternary SNAREs to zip up, uniting the vesicular and plasma membranes (Margittai et al., 1999; Sorensen et al., 2006). Other evidence suggests that ternary SNARE complex formation is a concerted process with more than one transition state during initial and sustained dilation of a protein fusion pore (Han and Jackson, 2006).

Despite the controversy with regards to the SNARE complex-mediated membrane fusion, widespread consensus holds that synaptotagmin is the  $\text{Ca}^{2+}$  sensor for stimulated exocytosis and may provide the cue for full fusion versus kiss-and-run fusion. Mutagenesis studies, for example, indicate that fusion is inhibited in the presence of synaptotagmin mutants with diminished SNARE interactions (Bai et al., 2004). Furthermore, over-expression of different isoforms of synaptotagmin in PC12 cells leads to different fusion pore opening durations, suggesting that the interaction of synaptotagmin with the SNARE complex and the membrane impacts the nature of fusion pore formation and dilation (Wang et al., 2001).  $\text{G}\beta\gamma$  signaling is another mediator of fusion pore dynamics (Blackmer et al., 2005; Chen et al., 2005; Gerachshenko et al., 2005; Photowala et al., 2006), but it is unclear how the  $\text{Ca}^{2+}$ -dependent synaptotagmin/SNARE complex interaction is actively modulated by  $\text{G}\beta\gamma$  (Searl and Silinsky, 2005).

We have shown recently that the nine C-terminal residues of SNAP25 that interact with synaptotagmin provide an important binding site for  $\text{G}\beta\gamma$ . The resulting  $\text{G}\beta\gamma$ /SNARE interaction inhibits transmitter release in vertebrate central synapses and mammalian neuroendocrine cells (Blackmer et al., 2005; Gerachshenko et al., 2005). We now identify  $\text{G}\beta\gamma$  binding sites on the SNARE complex. Additionally, we identify a role for  $\text{Ca}^{2+}$  and demonstrate competition between  $\text{G}\beta\gamma$  and synaptotagmin for binding to SNARE complexes. We propose that modulation of exocytosis is subject to convergent and complementary pathways directed to alteration of

synaptotagmin/SNARE complex interactions in which presynaptic  $\text{Ca}^{2+}$  both stimulates fusion and modifies the impact of Gi/o-coupled inhibitory GPCRs on exocytosis.

## Materials and Methods

### Plasmids

The open reading frames for the SNARE component proteins were sub-cloned into the pGEX6p1 vector (Amersham) for expression in bacteria. Individual truncation mutants were generated via a PCR-based strategy.

### SNARE protein purification

Recombinant bacterially-expressed glutathione S-transferase fusion proteins were expressed in *Escherichia coli* strain BL21(DE3). Protein expression was induced with 0.1 mM isopropyl  $\beta$ -D-thiogalactoside for 16 hr at room temperature. Bacterial cultures were pelleted, washed with 1 $\times$ PBS and then resuspend in lysis buffer {50 mM NaCl, 50 mM Tris, pH 8.0, 5 mM EDTA, 0.1% TritonX-100, 2 mM PMSF, and 1 mM dithiothreitol (DTT)}. Cells were lysed with a sonic dismembrator at 4 °C. GST-SNAP25 and GST-VAMP2 were purified from cleared lysates by affinity chromatography on glutathione–agarose (Pharmacia), following the manufacturer's instructions. While the proteins were bound to the column, the buffer was exchanged to 20 mM HEPES, pH 7.4, 100 mM NaCl, 0.05% n-octyl  $\beta$ -D-glucopyranoside (OG) and 5 mM dithiothreitol. In some cases, the proteins were eluted by cleaving from GST with PreScission protease (GE Healthcare) for 4 hr at 4 °C and then dialysed extensively against 20 mM HEPES, pH 7.0, 80 mM KCl, 20 mM NaCl and 0.05% OG. GST-Syntaxin1A (lacking the transmembrane domain) was purified from the sonicated bacterial supernatant by affinity chromatography on

glutathione–agarose (Pharmacia) in 10 mM Hepes, pH 7.4, 0.05 % OG and 2 mM DTT. Protein concentrations were determined with a Bradford assay kit (Pierce), and purity was verified by SDS/PAGE analysis.

### **Binary and ternary SNARE complex reassembly**

An equimolar ratio (3  $\mu$ M) of GST-syntaxin1A on glutathione-agarose and SNAP25 were incubated overnight at 4 °C in 20 mM Hepes, pH 7.4, 100 mM NaCl, 0.1% OG and 2.0 mM dithiothreitol. The binary t-SNARE complex was washed three times with PBS and eluted from the column by removing GST with PreScission protease (GE healthcare) for 4 hr at 4 °C. Equimolar protein-protein interaction was confirmed by SDS-PAGE/Coomassie staining analysis. To reassemble ternary SNARE complex, an equimolar ratio (3  $\mu$ M) of GST-syntaxin1A on glutathione-agarose, VAMP2 and SNAP25 were incubated overnight at 4 °C in 20 mM Hepes, pH 7.4, 100 mM NaCl, 0.1% OG and 2.0 mM DTT. The SNARE proteins were washed and eluted from the column by removing GST. SDS- and heat-stable SNARE complex formation was verified by SDS/PAGE analysis with/without a 15 min incubation at 100 °C.

### **G $\beta$ $\gamma$ purification and labeling**

G $\beta$  $\gamma$ <sub>1</sub> was purified from bovine retina as previously described (Mazzoni et al., 1991). Recombinant G $\beta$  $\gamma$ <sub>2</sub> was expressed in Sf9 cells and purified via a His<sub>6</sub> tag on G $\gamma$ <sub>2</sub> using Ni-NTA affinity chromatography (Sigma Aldrich). Fluorescence labeling of G $\beta$  $\gamma$ <sub>1</sub> and binding assays were conducted as described (Phillips and Cerione, 1991). Briefly, purified G $\beta$  $\gamma$ <sub>1</sub> was dialyzed into labeling buffer (20 mM HEPES, pH 7.4, 5 mM MgCl<sub>2</sub>, 150 mM NaCl, 10% Glycerol), then mixed with 2-(4'-Maleimidylanilino) naphthalene-6-sulphonic acid (MIANS) in a 5-fold molar

excess. The reaction proceeded for 3 hr at 4 °C before quenching with 5 mM 2-mercaptoethanol. The MIANS-G $\beta_1\gamma_1$  complex was separated from unreacted MIANS using a PD-10 desalting column (GE Healthcare). MIANS- G $\beta_1\gamma_1$  was stored in aliquots at -80 °C.

### **Fluorescence binding and competition assay**

All fluorescence measurements were performed in a fluorescence spectrophotometer (Cary Eclipse) at room temperature. Generally, MIANS-G $\beta_1\gamma_1$  was diluted into 0.5 ml of assay buffer (20 mM HEPES, pH 7.5, 5 mM MgCl<sub>2</sub>, 1 mM DTT, 0.1 M NaCl, 1 mM EDTA) to a final concentration of 20 nM. The MIANS fluorescence was monitored at excitation 322 nm and emission 417 nm. All proteins purified as GST fusion proteins were cleaved from GST with PreScission protease (GE healthcare) prior to analysis. The fluorescent changes caused by the addition of SNARE complexes were monitored continuously. Note that the amplitude of the fluorescence increase is not a measure of the affinity of the complex, but rather reflects the specific site on fluorescently-labeled G $\beta\gamma$  of interaction with each protein. There was no non-specific binding of the free probe to the SNARE proteins and MIANS-G $\beta\gamma$  was resistant to photobleaching under experimental conditions (data not shown). For G $\beta\gamma$ /synaptotagmin competition assays, various concentrations of synaptotagmin with SNARE proteins were added to labeled G $\beta_1\gamma_1$  with the noted Ca<sup>2+</sup> concentrations, and fluorescence changes were monitored. The EC<sub>50</sub> concentrations were determined by sigmoidal curve fitting using GraphPad Prism.

### **GST pull down assay**

GST-SNAP25, GST-VAMP2 and GST-syntaxin1A (5  $\mu$ g of each protein) were incubated with various amount of G $\beta_1\gamma_2$  proteins for 1 hr at 4 °C and washed three times with assay buffer (20



mM Hepes, pH 7.0, 80 mM KCl, 20 mM NaCl and 0.1% OG). The complex was eluted with 20  $\mu$ l of SDS sample buffer followed by separation via SDS-PAGE. Precipitated G $\beta$  was detected using western blotting with a rabbit anti-pan G $\beta$  antibody (Santa Cruz, T-20).

### **Electrophysiology and microinjection**

Lamprey spinal cord preparations (*Petromyzon marinus*) were performed as previously described (Wickelgren, 1977). Whole-cell patch-clamp recordings were achieved with a modified blind technique (Blanton et al., 1989) using pipettes (5 to 10 M $\Omega$ ) containing solution of the following composition: 102.5 mM MeSO<sub>4</sub>, 1 mM NaCl, 1 mM MgCl<sub>2</sub>, 5 mM HEPES, 0.05 mM EGTA, brought to a pH of 7.4 with KOH. All paired recordings to measure the effect of protein injection in this study were made at a minimum of 5 min after injection and less than 100  $\mu$ m from the presynaptic injection site. Recombinant G $\beta$ <sub>1</sub> $\gamma$ <sub>2</sub> protein was stored at -20 °C in a solution containing 100 mM MeSO<sub>4</sub>, 5 mM HEPES, 0.05 mM EGTA at pH of 7.4. Concentrations ranged from 3 - 5 mg/ml. For microinjection into the presynaptic terminal, 50% by volume of 1 M KMeSO<sub>4</sub> was added to the G $\beta$ <sub>1</sub> $\gamma$ <sub>2</sub> containing solution. Protein was pressure microinjected through presynaptic microelectrodes using Picospritzer II.

### **Imaging**

Fluorescence images were recorded with a modified confocal microscope (Bio-Rad MRC600) run with custom software available at <http://alford.bios.uic.edu>. Reticulospinal axons were labeled retrogradely with a dextran amine-conjugate form of the Ca<sup>2+</sup>-sensitive dye Fluo-4 (high affinity; Molecular Probes). The dye was applied using a suction pipette fitted to the cut end, immediately after the end of the spinal cord was cut. The tissue was then incubated overnight for

the dye to be transported throughout the axons. Images were collected at high speed by scanning a laser over a single line at 500 Hz. Imaging data were analysed using ImageJ software on a Macintosh computer. ImageJ was used to calculate the brightness value (range of possible values, 10 bit) for each pixel in a field of view. For each individual axon of interest, the brightness values were measured, and after background subtraction, images were normalized to the baseline level of fluorescence to give  $(F+I)/F$  values.

### **Calibration of the Ca<sup>2+</sup> sensitive dyes**

The dye sensitivity to Ca<sup>2+</sup> was determined using the same optical path (confocal microscope) that was used to measure Ca<sup>2+</sup> transients in the tissue. Dyes (5 μM) were prepared in blends of two Ca<sup>2+</sup> buffer standards (10 mM K<sub>2</sub>EGTA, 100 mM KCl and 30 mM MOPS) and (10 mM CaEGTA, 100 mM KCl and 30 mM MOPS) both at pH 7.2 (Molecular Probes) to make an 11 point standard curve. The absolute Ca<sup>2+</sup> values of the mix were corrected for the low temperatures used in this study (10 °C). The dye buffer mix was placed between cover slips cooled from below with a liquid cooling system to 10 °C and imaged from above with the 40X water immersion lens.

Western blots are representative of at least three independent experiments. Data points are presented as mean ± SEM (\* indicates  $p < 0.01$  and \*\* indicates  $p < 0.001$ , two-tailed Student's t-test).

## Results

### **G $\beta\gamma$ interacts with individual SNARE proteins as well as ternary SNARE complex.**

To understand the relationship between G $\beta\gamma$  and the SNARE complex in the modulation of exocytosis, we characterized sites of interaction by two complementary *in vitro* approaches, GST pulldowns and fluorescent binding assays. In GST pulldowns, both components of the t-SNARE (syntaxin1A and SNAP25) interacted with G $\beta\gamma$  individually. Additionally, the vesicular SNARE component, VAMP2, was found to interact directly with G $\beta\gamma$  (Fig. 1B). To demonstrate that the GST pulldown assay provides specific binding, we performed pulldown assay with G $\alpha$  subunit and heterotrimeric G protein that contains G $\alpha\beta\gamma$ . The G $\beta\gamma$  subunit, but not the G $\alpha$  subunit or the heterotrimeric G proteins, interacts with SNARE proteins, suggesting that G protein interaction with SNARE occurs upon inhibitory G protein-coupled receptor activation that induces G $\alpha$  and G $\beta\gamma$  dissociation (supplementary figure S1).

To quantify the relative contributions to G $\beta\gamma$  binding by the individual SNARE components, we employed a sensitive and quantitative fluorescence assay for measuring protein-protein interactions (Phillips and Cerione, 1991). G $\beta_1\gamma_1$  was labeled with the environmentally-sensitive fluorescent probe MIANS. This probe serves to report interaction with a binding partner because it undergoes enhanced fluorescence when the local environment becomes more hydrophobic. In these assays, labeled G $\beta\gamma$  (final concentration 20 nM) was used, while interactions with different concentrations of individual SNARE proteins or complexes were assessed through fluorescence intensity changes. Therefore, apparent affinities were estimated by determining concentrations of binding proteins at which MIANS fluorescence reached 50% of maximum (EC<sub>50</sub>).

This assay was used to quantify the interaction of G $\beta\gamma$  with the ternary SNARE complex and its constituent proteins (Fig. 1C, D). The ternary SNARE complex indeed caused a dose-

dependent increase in the fluorescence of MIANS-G $\beta\gamma$ , consistent with our previous findings that G $\beta\gamma$  and the SNARE complex interact *in vitro* (Blackmer et al., 2005; Blackmer et al., 2001) (Fig. 1C, EC<sub>50</sub> = 0.27  $\mu$ M). Similarly, we tested the apparent G $\beta\gamma$ -binding affinities of the individual SNARE components (Fig. 1D). Each of the three components caused a fluorescence increase, confirming direct interactions. The relative affinities followed the order syntaxin1A (EC<sub>50</sub> = 0.33  $\mu$ M), VAMP2 (0.94  $\mu$ M) and SNAP25 (1.07  $\mu$ M).

### **G $\beta\gamma$ interacts with the syntaxin1A H3 motif and the C-terminus of SNAP25.**

Syntaxin1A has two major regions, the H3 SNARE domain and the modulatory Habc region (Fig. 2A). Truncation mutants representing the two major syntaxin1A regions were generated (Fig. 2A) and EC<sub>50</sub> values for binding to 20 nM MIANS-labeled G $\beta\gamma$  were determined. The syntaxin1A H3 domain showed a right-shifted binding curve (EC<sub>50</sub> = 0.89  $\mu$ M; Fig. 2B) relative to the entire molecule (EC<sub>50</sub> = 0.33  $\mu$ M). Syntaxin1A (1-190) did not induce a significant G $\beta\gamma$  fluorescence change. These results, which were confirmed by GST pulldown assays (data not shown), indicate that G $\beta\gamma$  binds to the syntaxin1A H3 SNARE domain. However, since G $\beta\gamma$  bound to the H3 domain with an affinity lower than for intact syntaxin1A, we cannot rule out a masked minor contribution of the Habc domain, or that the isolated domain does not fold optimally (Jarvis et al., 2002).

Recent evidence suggests that nine amino acids from the C-terminus of SNAP25 are crucial for interaction with G $\beta\gamma$  as well (Blackmer et al., 2005; Gerachshenko et al., 2005). BoNT/A treatment, which removes nine C-terminal residues of SNAP25 (SNAP25 $\Delta$ 9) (Fig. 2C), diminishes G $\beta\gamma$ -mediated inhibition of exocytosis (Blackmer et al., 2005; Gerachshenko et al., 2005). Additionally, a ternary SNARE complex comprising VAMP2, syntaxin1A and

SNAP25 $\Delta$ 9, shows reduced G $\beta\gamma$  binding compared to the wild type SNARE complex (Gerachshenko et al., 2005). Here, we quantified the direct interaction of G $\beta\gamma$  with the C-terminus of SNAP25. A truncation mutant of SNAP25 that mimics the BoNT/A cleavage product (SNAP25 $\Delta$ 9) was analyzed for its binding to G $\beta\gamma$ . Relative to full-length SNAP25, SNAP25 $\Delta$ 9 showed significantly decreased affinity for G $\beta\gamma$  (Fig. 2D).

In presynaptic terminals of neurons *in situ* and in cultured PC12 and chromaffin cells, BoNT/E, which cleaves 26 amino acids from the C-terminus of SNAP25 (Fig. 2C), inhibits Ca<sup>2+</sup>-dependent exocytosis (Chen et al., 2001; Ferrer-Montiel et al., 1998), consistent with an observed loss of interaction between synaptotagmin and SNAP25 (Chen et al., 1999; Gerona et al., 2000). We investigated whether a further truncated SNAP25 (SNAP25 $\Delta$ 26) also weakens binding to G $\beta\gamma$ . Fluorescent binding assays demonstrated that deletion of 26 amino acids caused a great loss of G $\beta\gamma$  binding (Fig. 2D). These data indicate that 26 C-terminal amino acids of SNAP25 are also critical for G $\beta\gamma$  binding.

### **G $\beta\gamma$ and synaptotagmin compete in binary- and ternary SNARE complexes in a Ca<sup>2+</sup>-dependent manner.**

Interestingly, the G $\beta\gamma$ -binding domains of the SNARE complex, the syntaxin1A H3 domain and the C-terminus of SNAP25, are also known to constitute functionally important Ca<sup>2+</sup>-dependent synaptotagmin binding sites (Chapman et al., 1995; Gerona et al., 2000). The overlapping of binding sites suggests that there might be competition between G $\beta\gamma$  and synaptotagmin on the complexed SNAREs. To test whether G $\beta\gamma$  competes with synaptotagmin for binding to SNARE proteins in complex, we conducted competition assays *in vitro*. We used a mutant of synaptotagmin I (K326A, K327A) that exhibits wild-type SNARE binding affinity but

holds a reduced propensity to oligomerize and to form insoluble aggregates in response to high concentrations of  $\text{Ca}^{2+}$  (Bai et al., 2004). In fluorescent binding assays, synaptotagmin does not interact significantly with MIANS- $\text{G}\beta\gamma$  (data not shown). We therefore tested competition between  $\text{G}\beta\gamma$  and synaptotagmin for binding to the binary t-SNARE complex, comprising syntaxin1A and SNAP25. The interaction between  $\text{G}\beta\gamma$  and binary t-SNARE complex in the absence of synaptotagmin was normalized to 100%. In 50  $\mu\text{M}$   $\text{Ca}^{2+}$ , the interaction between MIANS- $\text{G}\beta\gamma$  and 1  $\mu\text{M}$  binary t-SNARE complex was almost completely inhibited by 250 nM synaptotagmin I (Fig. 3A). Increasing synaptotagmin concentrations competed more effectively with  $\text{G}\beta\gamma$ , resulting in reduced fluorescence changes (Fig. 3B), further indicating that  $\text{G}\beta\gamma$  and synaptotagmin compete for SNARE binding.

Synchronous vesicle fusion is initiated by  $\text{Ca}^{2+}$ , but additional  $\text{Ca}^{2+}$  influx may modify large dense core fusion properties and possibly alter the quantal size of synaptic neurotransmitter release (Elhamdani et al., 2006; Elhamdani et al., 2001; Harata et al., 2006). Since this modulation may reflect the  $\text{Ca}^{2+}$  sensitivity of synaptotagmin (Morimoto et al., 1995), we tested whether competition with  $\text{G}\beta\gamma$  is also  $\text{Ca}^{2+}$  sensitive. We found that the competition between synaptotagmin and  $\text{G}\beta\gamma$  for binary t-SNARE complex binding is dependent on intracellular  $\text{Ca}^{2+}$  concentrations. In buffer lacking  $\text{Ca}^{2+}$ , synaptotagmin caused a slight but statistically significant inhibition of the ability of t-SNAREs to increase the fluorescence of MIANS- $\text{G}\beta\gamma$  (Fig. 3C), possibly due to a limited  $\text{Ca}^{2+}$ -independent interaction between synaptotagmin and t-SNAREs (Bennett et al., 1992; Sollner et al., 1993). However, upon addition of physiologically relevant concentrations of  $\text{Ca}^{2+}$ , we observed an increased inhibition of  $\text{G}\beta\gamma$  binding by synaptotagmin, with maximum effectiveness at 50  $\mu\text{M}$   $\text{Ca}^{2+}$  (Fig. 3C).

Interactions of both G $\beta\gamma$  and synaptotagmin with the ternary SNARE complex modify the dilation of the vesicle fusion pore (Bai et al., 2004; Photowala et al., 2006). Thus, we tested the hypothesis that G $\beta\gamma$  competes with synaptotagmin for binding to the ternary SNARE complex. We first measured the G $\beta\gamma$ /SNARE interaction by determining the change in fluorescence of 20 nM MIANS-G $\beta\gamma$  upon addition of the ternary SNARE complex. Addition of 1  $\mu$ M SNARE complex induced an increase of fluorescence intensity (Fig. 3D). This increase was reduced by inclusion of 250 nM synaptotagmin, indicating that G $\beta\gamma$  and synaptotagmin compete for binding to the ternary SNARE complex. Additionally, competition by synaptotagmin and the resulting reduced fluorescence changes were dependent on the concentration of synaptotagmin (Fig. 3E) and the concentration of Ca<sup>2+</sup> (Fig. 3F). Together, these data suggest that indeed G $\beta\gamma$  and synaptotagmin compete for binding to the ternary SNARE complex.

### **G $\beta\gamma$ and synaptotagmin compete for binding to the individual t-SNARES (syntaxin 1A and SNAP25) but not the v-SNARE (VAMP2).**

The H3 domain of syntaxin1A and the C-terminus of SNAP25 provide interaction regions for G $\beta\gamma$  and synaptotagmin. Interestingly, we saw significantly more efficient competition between G $\beta\gamma$  and synaptotagmin in the context of binary t-SNAREs than ternary SNARE complexes. Therefore, we measured the individual contributions of SNARE components to competition between G $\beta\gamma$  and synaptotagmin.

First, to determine if G $\beta\gamma$  and synaptotagmin compete for binding to syntaxin1A or SNAP25, the interaction of 20 nM of MIANS-G $\beta\gamma$  with syntaxin1A and SNAP25 was monitored with or without preincubation of the SNARE proteins with 20 nM synaptotagmin. The interactions between G $\beta\gamma$  and SNARE proteins were unaffected by Ca<sup>2+</sup> in the absence of synaptotagmin

(data not shown). In the absence of  $\text{Ca}^{2+}$ , we observed a slight, statistically insignificant decrease in  $\text{G}\beta\gamma$  binding to both syntaxin1A (Fig. 4A) and SNAP25 (Fig. 4B) upon preincubation of the SNARE proteins with 20 nM synaptotagmin. However, in 100  $\mu\text{M}$   $\text{Ca}^{2+}$ , the ability of synaptotagmin to compete for binding to SNAREs was greatly enhanced. Syntaxin1A binding to  $\text{G}\beta\gamma$  was reduced by 48% (Fig. 4A), and binding of SNAP25 to  $\text{G}\beta\gamma$  was reduced by 78% (Fig. 4B). Thus,  $\text{G}\beta\gamma$  competes with  $\text{Ca}^{2+}$ -synaptotagmin for binding to both syntaxin1A and SNAP25.

We observed a direct interaction between  $\text{G}\beta\gamma$  and VAMP2 (Fig. 1B and D). An earlier study suggested that synaptotagmin interacts with VAMP2 (Fukuda, 2002), leading to the possibility that this protein forms an additional site of competition between  $\text{G}\beta\gamma$  and synaptotagmin. However, the existence of a direct synaptotagmin/VAMP2 interaction remains controversial (Chapman et al., 1995). Consequently, we monitored the  $\text{G}\beta\gamma$  interaction with VAMP2 with or without preincubation of VAMP2 with synaptotagmin in the presence or absence of  $\text{Ca}^{2+}$ . No alteration in  $\text{G}\beta\gamma$  binding to VAMP2 by synaptotagmin was observed, suggesting that  $\text{G}\beta\gamma$  and synaptotagmin do not share a binding region on VAMP2 (Fig. 4C). This result may explain why competition at the ternary SNARE complex appears to favor  $\text{G}\beta\gamma$  binding as compared to competition at the binary t-SNARE: in the ternary SNARE complex,  $\text{G}\beta\gamma$  binding is enhanced by an additional binding site within VAMP2 that is unaffected by synaptotagmin I. Thus its ability to compete with  $\text{G}\beta\gamma$  in the ternary SNARE complex is decreased.

### **The C-terminus of SNAP25 in the ternary SNARE complex is important for $\text{G}\beta\gamma$ -synaptotagmin competition.**

Previously, we showed that botulinum toxin A (BoNT/A), which specifically removes the C-terminal nine amino acids from SNAP25, greatly reduced the inhibitory effect of  $\text{G}\beta\gamma$  on



regulated exocytosis (Blackmer et al., 2001; Gerachshenko et al., 2005). We propose that this reduction can be explained if removal of these residues diminishes G $\beta\gamma$  competition with synaptotagmin for binding to the t-SNAREs and the ternary SNARE complex *in vivo*. Therefore, we examined the contribution of the C-terminus of SNAP25 in the competition between G $\beta\gamma$  and synaptotagmin within the ternary SNARE complex. Importantly, while BoNT/A cleavage of SNAP25 reduced binding of synaptotagmin and G $\beta\gamma$  individually, significant interactions were still observed (Fig. 2D). Thus, it was important to quantify the interactions using the fluorescent binding assay to determine if this cleavage shifted the G $\beta\gamma$ /synaptotagmin competition towards synaptotagmin binding.

To test the relative contributions of the C-terminus of SNAP25 in binding G $\beta\gamma$  and synaptotagmin, we quantified binding to ternary SNARE complexes comprising syntaxin1A, VAMP2 and SNAP25 $\Delta$ 9. Competition by synaptotagmin for G $\beta\gamma$  binding to SNARE complex that contains SNAP25 $\Delta$ 9 was increased compared to the wild type SNARE complex at 50  $\mu$ M of Ca<sup>2+</sup> (Fig. 5A). This finding is consistent with a model in which the nine C-terminal amino acids of SNAP25 represent an important determinant mediating exclusion of synaptotagmin binding by G $\beta\gamma$ .

We then determined the concentration dependence of the synaptotagmin competition. The strength of synaptotagmin competition in SNARE complexes formed with SNAP25 $\Delta$ 9 increased dramatically compared to the wild type SNARE complex (Fig. 5B). These results suggest that the C-terminal nine amino acids of SNAP25 are more critical for G $\beta\gamma$  than for synaptotagmin binding. These data support the dramatic loss of inhibitory effect of G $\beta\gamma$  in the BoNT/A treated synapse (Gerachshenko et al., 2005).

## **The 5-HT mediated regulation of exocytosis is diminished with high $[Ca^{2+}]$ at the lamprey giant synapse.**

What role does  $G\beta\gamma$ -synaptotagmin I competition for SNARE complexes play at synapses? At lamprey giant synapses, we have showed that 5-HT inhibits transmitter release through direct  $G\beta\gamma$ /SNARE complex interactions. 5-HT mediated  $G\beta\gamma$  does not inhibit voltage gated  $Ca^{2+}$  channels in this preparation, but directly acts on the ternary SNARE complex to inhibit exocytosis (Blackmer et al., 2001; Gerachshenko et al., 2005; Takahashi et al., 2001). From our *in vitro* study we hypothesize that  $G\beta\gamma$ -mediated inhibition requires competition between  $G\beta\gamma$  and  $Ca^{2+}$ -dependent synaptotagmin binding on the SNARE complex. These findings suggest that the effect of GPCR-mediated activation of  $G\beta\gamma$  will be mitigated by raising the synaptic terminal  $Ca^{2+}$  concentration.

We tested this possibility using paired recordings between giant axons and postsynaptic neurons in lamprey synapse. To increase action potential-evoked intracellular  $Ca^{2+}$  concentrations, we raised extracellular  $Ca^{2+}$  concentrations (Fig. 6A-C). We first quantified the consequent effect on evoked presynaptic  $Ca^{2+}$  entry. Axons were filled with a  $Ca^{2+}$  sensitive dye (Fluo-4 dextran high affinity) and imaged with confocal microscopy. Action potential-evoked presynaptic fluorescence transients were imaged under increasing extracellular  $Ca^{2+}$  (2.6 mM, 10 mM and 50 mM; Fig. 6B-C and data not shown). The relationship between extracellular  $Ca^{2+}$  concentrations and the fluorescence transient was alinear (Fig. 6E). Therefore, to calculate the relationship between extracellular  $Ca^{2+}$  and the intracellular  $Ca^{2+}$  transient amplitude we determined the peak intracellular  $Ca^{2+}$  during the transients. The affinity of the dye (1.2  $\mu$ M) was obtained from fluorescence curves that showed a 120-fold increase in fluorescence between 0  $\mu$ M  $Ca^{2+}$  and saturation (41  $\mu$ M) at a physiological temperature. Using these data and the resting

[Ca<sup>2+</sup>] in lamprey axons (approximately 100 nM), we estimated the peak transient intracellular Ca<sup>2+</sup> (Fig. 6E). 50 mM extracellular Ca<sup>2+</sup> slightly increased basal presynaptic intracellular Ca<sup>2+</sup> (Fig. 6D). However, the evoked fluorescence transient, and therefore its peak Ca<sup>2+</sup> concentration, was markedly increased (Fig. 6E). Note that absolute Ca<sup>2+</sup> concentrations calculated in this way underestimate the concentration at the vesicle fusion site because we cannot image with sufficient resolution to resolve the close spatial relationship between Ca<sup>2+</sup> channels and the release machinery (Adler et al., 1991). Consequently, we used these data to calculate the relative amplitude of the Ca<sup>2+</sup> transient at extracellular concentrations of 10 and 50 mM (Fig. 6F) normalized to control (2.6 mM).

We then tested the effect of increased Ca<sup>2+</sup> on 5-HT-mediated presynaptic inhibition. At a control extracellular Ca<sup>2+</sup> concentration (2.6 mM), 5-HT (600 nM) reduced the EPSC to 55.9±7.3% of control (n=5; P<0.05). The EPSC fully recovered upon 5-HT removal (Fig. 7A, top). 50 mM extracellular Ca<sup>2+</sup> increased the EPSC amplitude to 129.7±4.7% of control (n=5; P<0.01), but 600 nM 5-HT caused no inhibition (Fig. 7A, bottom; EPSC was 97.1±8.1% of the EPSC modified by 50 mM Ca<sup>2+</sup>; n=5 pairs). At 50 mM extracellular Ca<sup>2+</sup>, even a saturating dose of 5-HT (10 μM) resulted in only a slight reduction in the EPSC {response was 71.3±0.9% of the control response modified by high Ca<sup>2+</sup> (n=3, P>0.05), compared to a reduction to 20% of control in normal Ca<sup>2+</sup> (Takahashi et al., 2001)} (Fig. 7B and C). We also confirmed that 5-HT does not change Ca<sup>2+</sup> influx in lamprey synapses (Blackmer et al., 2001; Takahashi et al., 2001) treated with 50 mM extracellular Ca<sup>2+</sup> concentration (supplementary figure S2). Thus, increased intracellular Ca<sup>2+</sup> transients attenuated GPCR mediated presynaptic inhibition.

**High extracellular Ca<sup>2+</sup> attenuates the presynaptic inhibitory effect of Gβγ.**

We have shown that the reduction of the EPSC upon activation of 5-HT receptors is caused by liberated G $\beta\gamma$  (Blackmer et al., 2001; Gerachshenko et al., 2005). Here, we examined the effects of manipulating intracellular Ca<sup>2+</sup> on EPSC inhibition by free G $\beta\gamma$  introduced through direct injection of purified G $\beta\gamma$  protein into presynaptic axons. We compared G $\beta\gamma$ -mediated inhibition of exocytosis at a control (2.6 mM) and a raised Ca<sup>2+</sup> concentration (10 mM). 10 mM Ca<sup>2+</sup> increased the EPSC amplitude (Fig. 8A; to 122±2% of control, n=3). In four more paired recordings we probed the effect of raising Ca<sup>2+</sup> concentrations on inhibition by presynaptic G $\beta\gamma$ . In control Ca<sup>2+</sup> (2.6 mM), G $\beta\gamma$  injection significantly reduced the EPSC as previously described (Blackmer et al., 2001) (to 37±12%; Fig. 8B and C). In the same pairs the Ca<sup>2+</sup> concentration was raised to 10 mM and G $\beta\gamma$  inhibition was reversed (10 mM; Fig. 8B, C; EPSC was 100±9% of control). Thus raised Ca<sup>2+</sup> transient amplitudes significantly attenuated the inhibitory effect of presynaptic G $\beta\gamma$ . The effects of both 5-HT and presynaptic G $\beta\gamma$  injection are attenuated by enhancing the amplitude of the action potential evoked presynaptic Ca<sup>2+</sup> transient.

## Discussion

In primed vesicles, Ca<sup>2+</sup> effects exocytosis in part by increasing synaptotagmin's affinity for the primed SNARE complex (Bai et al., 2004; Perin et al., 1990; Schiavo et al., 1997; Wang et al., 2006; Yoshihara and Littleton, 2002). G $\beta\gamma$  liberated by inhibitory Gi/o-coupled GPCRs inhibits neurotransmitter release by at least two mechanisms: inhibition of presynaptic Ca<sup>2+</sup> entry at many synapses by modulating voltage-gated calcium channels (Herlitze et al., 1996; Ikeda, 1996), as well as interaction with the ternary SNARE complex late in membrane fusion (Blackmer et al., 2005; Gerachshenko et al., 2005). Here we show that G $\beta\gamma$  interacts with SNARE proteins and that this binding is not directly modified by calcium. G $\beta\gamma$  interacts with

VAMP2 at a site different from synaptotagmin's interaction. Perhaps the G $\beta\gamma$ /VAMP2 interaction strengthens G $\beta\gamma$  binding to the SNARE complex while occlusion of synaptotagmin I binding occurs through the t-SNARE components (syntaxin1A and SNAP25) in the ternary SNARE complex. In addition, G $\beta\gamma$  binds directly to the t-SNAREs SNAP25 and syntaxin1A at similar sites to those synaptotagmin uses to interact with these proteins in a Ca<sup>2+</sup>-dependent manner. This sets up a potent competition with the Ca<sup>2+</sup> sensor to inhibit regulated exocytosis. This differential Ca<sup>2+</sup> requirement can lead to a Ca<sup>2+</sup>-sensitivity of the G $\beta\gamma$  inhibition of SNARE/synaptotagmin complex formation: at low and moderate Ca<sup>2+</sup> concentrations, the presence of inhibitory signals generates G $\beta\gamma$  that competes with synaptotagmin for binding to SNARE, leading to inhibition of exocytosis. At high Ca<sup>2+</sup> concentrations, the affinity of synaptotagmin for SNARE increases while the G $\beta\gamma$ /SNARE affinity remains steady, and thus high synaptic activity overrides the inhibition by G $\beta\gamma$ .

At the synapse, after C-terminal truncation of SNAP-25 with BoNT/A, exocytosis recovers in high Ca<sup>2+</sup> in many preparations, including the lamprey (Gerachshenko et al., 2005), presumably because high Ca<sup>2+</sup> enhances the residual synaptotagmin/SNARE interaction that remains after BoNT/A treatment. However, the affinity of G $\beta\gamma$  for the modified SNARE complex is much lower, and G $\beta\gamma$  therefore competes less well with synaptotagmin for the same site, particularly at raised intracellular Ca<sup>2+</sup>. These findings led to a testable hypothesis: at the synapse, larger evoked Ca<sup>2+</sup> transients should prevent G $\beta\gamma$ -mediated presynaptic inhibition induced by 5-HT. Accordingly, in the lamprey giant synapse, while 5-HT powerfully inhibits exocytosis through G $\beta\gamma$  interaction with the SNARE complex (Blackmer et al., 2005; Blackmer et al., 2001; Chen et al., 2005; Gerachshenko et al., 2005; Man-Son-Hing et al., 1989; Silinsky, 1984; Takahashi et al., 2001), we observed that enhancing the Ca<sup>2+</sup> transient reversed this inhibition (Fig. 6-7). These

data are consistent with the biochemical results showing that inhibition of synaptotagmin/SNARE complex interaction by  $G\beta\gamma$  is sensitive to  $Ca^{2+}$ . Though  $Ca^{2+}$  could have other effects in the synapse, the fact that synaptotagmin is thought to be the major  $Ca^{2+}$  receptor for exocytosis (Bai et al., 2004; Maximov and Sudhof, 2005; Wang et al., 2006) suggests that  $G\beta\gamma$  may work physiologically by competing with  $Ca^{2+}$ -synaptotagmin for SNARE, leading to inhibition of exocytosis.  $G\beta\gamma$  also has many other targets, and enhancing intracellular  $Ca^{2+}$  could modify the effects of these interactions on exocytosis. The most obvious other  $G\beta\gamma$  effector is the voltage-gated  $Ca^{2+}$  channel, which has been shown by many investigators to be inhibited by  $G\beta\gamma$ . However,  $G\beta\gamma$  has no effect on  $Ca^{2+}$  entry even at 50 mM extracellular  $Ca^{2+}$ , as 5-HT does not modify evoked  $Ca^{2+}$  entry (supplementary figure S2).

This  $Ca^{2+}$ -dependent regulation may complete a physiological feedback loop, since  $G\beta\gamma$  may control both  $Ca^{2+}$  influx through voltage-gated  $Ca^{2+}$  channels (Herlitze et al., 1996; Ikeda, 1996) and access of the  $Ca^{2+}$  effector synaptotagmin to its site on the SNARE. Our data suggest that this competition is elegantly controlled by overlap of the binding sites of  $G\beta\gamma$  and synaptotagmin at the SNARE proteins SNAP25 and syntaxin. In a further level of regulation, during repetitive stimulation, buildup of intracellular  $Ca^{2+}$  concentration may reverse  $G\beta\gamma$  inhibition. Thus, depending on presynaptic Gi/o-coupled GPCR activation and  $Ca^{2+}$  influx in response to synaptic activity, there potentially exists a range of efficiencies of exocytosis. Thus we predict that a complex and dynamic regulation of vesicle fusion properties will occur. Finally, at low levels of inhibitory GPCR signaling,  $G\beta\gamma$  causes kiss-and-run exocytosis in lamprey synapses (Photowala et al., 2006) and adrenal chromaffin cells (data not shown) (Chen et al., 2005). In hippocampal neurons, sustained stimulus trains forcing high presynaptic  $Ca^{2+}$  concentrations change fusion from a state dominated by kiss-and-run to one favoring full fusion (Harata et al., 2006).

However, the exact  $\text{Ca}^{2+}$  concentrations required to reverse  $\text{G}\beta\gamma$ -mediated presynaptic inhibition are likely to exceed those obtained by residual  $\text{Ca}^{2+}$  during short bursts of stimuli, in which saturating doses of 5-HT remains effective (Takahashi et al., 2001). Thus we speculate that the dynamic relationship between inhibitory GPCRs and presynaptic  $\text{Ca}^{2+}$  constantly modifies the nature of the vesicle fusion event itself.

**Acknowledgements:** We thank Dr. T. F. Martin (University of Wisconsin) for the synaptotagmin C2AB cDNA, Dr. K. PM. Currie, Dr. A. Preininger and Dr. C. Wells (Vanderbilt University) and Dr. T Blackmer (Oregon Health Sciences University) for helpful discussions.

## Reference

- Adler EM, Augustine GJ, Duffy SN and Charlton MP (1991) Alien intracellular calcium chelators attenuate neurotransmitter release at the squid giant synapse. *J Neurosci* **11**:1496-507.
- Bai J, Wang CT, Richards DA, Jackson MB and Chapman ER (2004) Fusion pore dynamics are regulated by synaptotagmin<sup>\*</sup>-SNARE interactions. *Neuron* **41**:929-42.
- Bennett MK, Calakos N and Scheller RH (1992) Syntaxin: a synaptic protein implicated in docking of synaptic vesicles at presynaptic active zones. *Science* **257**:255-9.
- Blackmer T, Larsen EC, Bartleson C, Kowalchuk JA, Yoon EJ, Preininger AM, Alford S, Hamm HE and Martin TF (2005) G protein betagamma directly regulates SNARE protein fusion machinery for secretory granule exocytosis. *Nat Neurosci* **8**:421-5.
- Blackmer T, Larsen EC, Takahashi M, Martin TF, Alford S and Hamm HE (2001) G protein betagamma subunit-mediated presynaptic inhibition: regulation of exocytotic fusion downstream of Ca<sup>2+</sup> entry. *Science* **292**:293-7.
- Blanton MG, Lo Turco JJ and Kriegstein AR (1989) Whole cell recording from neurons in slices of reptilian and mammalian cerebral cortex. *J Neurosci Methods* **30**:203-10.
- Chapman ER, Hanson PI, An S and Jahn R (1995) Ca<sup>2+</sup> regulates the interaction between synaptotagmin and syntaxin 1. *J Biol Chem* **270**:23667-71.
- Chen XK, Wang LC, Zhou Y, Cai Q, Prakriya M, Duan KL, Sheng ZH, Lingle C and Zhou Z (2005) Activation of GPCRs modulates quantal size in chromaffin cells through G(betagamma) and PKC. *Nat Neurosci* **8**:1160-8.
- Chen YA, Scales SJ, Jagath JR and Scheller RH (2001) A discontinuous SNAP-25 C-terminal coil supports exocytosis. *J Biol Chem* **276**:28503-8.
- Chen YA, Scales SJ, Patel SM, Doung YC and Scheller RH (1999) SNARE complex formation is triggered by Ca<sup>2+</sup> and drives membrane fusion. *Cell* **97**:165-74.
- Elhamdani A, Azizi F and Artalejo CR (2006) Double patch clamp reveals that transient fusion (kiss-and-run) is a major mechanism of secretion in calf adrenal chromaffin cells: high calcium shifts the mechanism from kiss-and-run to complete fusion. *J Neurosci* **26**:3030-6.
- Elhamdani A, Palfrey HC and Artalejo CR (2001) Quantal size is dependent on stimulation frequency and calcium entry in calf chromaffin cells. *Neuron* **31**:819-30.
- Ferrer-Montiel AV, Gutierrez LM, Aplan JP, Canaves JM, Gil A, Viniegra S, Biser JA, Adler M and Montal M (1998) The 26-mer peptide released from SNAP-25 cleavage by botulinum neurotoxin E inhibits vesicle docking. *FEBS Lett* **435**:84-8.
- Fukuda M (2002) Vesicle-associated membrane protein-2/synaptobrevin binding to synaptotagmin I promotes O-glycosylation of synaptotagmin I. *J Biol Chem* **277**:30351-8.
- Gerachshenko T, Blackmer T, Yoon EJ, Bartleson C, Hamm HE and Alford S (2005) Gbetagamma acts at the C terminus of SNAP-25 to mediate presynaptic inhibition. *Nat Neurosci* **8**:597-605.
- Gerona RR, Larsen EC, Kowalchuk JA and Martin TF (2000) The C terminus of SNAP25 is essential for Ca<sup>(2+)</sup>-dependent binding of synaptotagmin to SNARE complexes. *J Biol Chem* **275**:6328-36.
- Han X and Jackson MB (2006) Structural transitions in the synaptic SNARE complex during Ca<sup>2+</sup>-triggered exocytosis. *J Cell Biol* **172**:281-93.



- Harata NC, Choi S, Pyle JL, Aravanis AM and Tsien RW (2006) Frequency-dependent kinetics and prevalence of kiss-and-run and reuse at hippocampal synapses studied with novel quenching methods. *Neuron* **49**:243-56.
- Herlitze S, Garcia DE, Mackie K, Hille B, Scheuer T and Catterall WA (1996) Modulation of Ca<sup>2+</sup> channels by G-protein beta gamma subunits. *Nature* **380**:258-62.
- Ikeda SR (1996) Voltage-dependent modulation of N-type calcium channels by G-protein beta gamma subunits. *Nature* **380**:255-8.
- Jarvis SE, Barr W, Feng ZP, Hamid J and Zamponi GW (2002) Molecular determinants of syntaxin 1 modulation of N-type calcium channels. *J Biol Chem* **277**:44399-407.
- Man-Son-Hing H, Zoran MJ, Lukowiak K and Haydon PG (1989) A neuromodulator of synaptic transmission acts on the secretory apparatus as well as on ion channels. *Nature* **341**:237-9.
- Margittai M, Otto H and Jahn R (1999) A stable interaction between syntaxin 1a and synaptobrevin 2 mediated by their transmembrane domains. *FEBS Lett* **446**:40-4.
- Maximov A and Sudhof TC (2005) Autonomous function of synaptotagmin 1 in triggering synchronous release independent of asynchronous release. *Neuron* **48**:547-54.
- Mazzoni MR, Malinski JA and Hamm HE (1991) Structural analysis of rod GTP-binding protein, Gt. Limited proteolytic digestion pattern of Gt with four proteases defines monoclonal antibody epitope. *J Biol Chem* **266**:14072-81.
- Morimoto T, Popov S, Buckley KM and Poo MM (1995) Calcium-dependent transmitter secretion from fibroblasts: modulation by synaptotagmin I. *Neuron* **15**:689-96.
- Perin MS, Fried VA, Mignery GA, Jahn R and Sudhof TC (1990) Phospholipid binding by a synaptic vesicle protein homologous to the regulatory region of protein kinase C. *Nature* **345**:260-3.
- Phillips WJ and Cerione RA (1991) Labeling of the beta gamma subunit complex of transducin with an environmentally sensitive cysteine reagent. Use of fluorescence spectroscopy to monitor transducin subunit interactions. *J Biol Chem* **266**:11017-24.
- Photowala H, Blackmer T, Schwartz E, Hamm HE and Alford S (2006) G protein beta{gamma}-subunits activated by serotonin mediate presynaptic inhibition by regulating vesicle fusion properties. *Proc Natl Acad Sci U S A* **103**:4281-6.
- Rizo J, Chen X and Arac D (2006) Unraveling the mechanisms of synaptotagmin and SNARE function in neurotransmitter release. *Trends Cell Biol.*
- Schiavo G, Stenbeck G, Rothman JE and Sollner TH (1997) Binding of the synaptic vesicle v-SNARE, synaptotagmin, to the plasma membrane t-SNARE, SNAP-25, can explain docked vesicles at neurotoxin-treated synapses. *Proc Natl Acad Sci U S A* **94**:997-1001.
- Searl TJ and Silinsky EM (2005) Modulation of Ca(2+)-dependent and Ca(2+)-independent miniature endplate potentials by phorbol ester and adenosine in frog. *Br J Pharmacol* **145**:954-62.
- Silinsky EM (1984) On the mechanism by which adenosine receptor activation inhibits the release of acetylcholine from motor nerve endings. *J Physiol* **346**:243-56.
- Sollner T, Bennett MK, Whiteheart SW, Scheller RH and Rothman JE (1993) A protein assembly-disassembly pathway in vitro that may correspond to sequential steps of synaptic vesicle docking, activation, and fusion. *Cell* **75**:409-18.
- Sorensen JB, Wiederhold K, Muller EM, Milosevic I, Nagy G, de Groot BL, Grubmuller H and Fasshauer D (2006) Sequential N- to C-terminal SNARE complex assembly drives priming and fusion of secretory vesicles. *Embo J.*

- Takahashi M, Freed R, Blackmer T and Alford S (2001) Calcium influx-independent depression of transmitter release by 5-HT at lamprey spinal cord synapses. *J Physiol* **532**:323-36.
- Wang CT, Bai J, Chang PY, Chapman ER and Jackson MB (2006) Synaptotagmin-Ca<sup>2+</sup> triggers two sequential steps in regulated exocytosis in rat PC12 cells: fusion pore opening and fusion pore dilation. *J Physiol* **570**:295-307.
- Wang CT, Grishanin R, Earles CA, Chang PY, Martin TF, Chapman ER and Jackson MB (2001) Synaptotagmin modulation of fusion pore kinetics in regulated exocytosis of dense-core vesicles. *Science* **294**:1111-5.
- Wickelgren WO (1977) Physiological and anatomical characteristics of reticulospinalneurons in lamprey. *J Physiol* **270**:89-114.
- Yoshihara M and Littleton JT (2002) Synaptotagmin I functions as a calcium sensor to synchronize neurotransmitter release. *Neuron* **36**:897-908.

## **Footnotes**

This work was supported by National Institutes of Health Grants EY10291 to HEH, MH64763 to SA and American Heart Associate predoctoral fellowship to EJY.

## Figure legends

**Fig. 1 G $\beta\gamma$  binds individual SNARE proteins and their ternary complex.** (A) *The SNAREs in the primed state and their relationship to synaptotagmin.* We hypothesize that G $\beta\gamma$  counteracts synaptotagmin by interacting with the C-terminal region of the SNARE complex. (B) *G $\beta\gamma$  interacts with SNAP25 and syntaxin1A in a GST pulldown assay (upper panel).* Equimolar amounts of GST (lane 1), GST-SNAP25 (lanes 2-4), or GST-syntaxin1A (lanes 5-7) were incubated with the noted concentrations of G $\beta_1\gamma_2$ . Precipitated G $\beta$  was detected with an anti-pan G $\beta$  antibody. Purified G $\beta\gamma$  was included as a loading control (lane 8). *G $\beta\gamma$  interacts directly with VAMP2 (bottom panel), {GST (lane 1), GST-VAMP2 (lanes 2-5 and lane a G $\beta\gamma$  loading control (lane 6)}.* (C) *Quantification of the interaction of G $\beta\gamma$  with the ternary SNARE complex with fluorescent binding.* Purified G $\beta\gamma$  was labeled with MIANS environmental sensitive fluorescence probe. The fluorescence change was monitored by spectrofluorometry using 20 nM labeled G $\beta\gamma$  and various concentrations of SNARE complex. Fluorescence change was normalized by basal level of labeled G $\beta\gamma$  fluorescence and represented as relative fluorescence. Increasing concentrations of the SNARE complex induced enhanced fluorescence of MIANS-G $\beta_1\gamma_1$ , indicating formation of a G $\beta\gamma$ /SNARE interaction. The data presented ratio of relative fluorescence (RF) at each different protein concentration (n = 3). (D) *Affinities of individual SNARE components for G $\beta\gamma$ .* Using the fluorescent binding assay, strengths of binding to 20 nM MIANS-G $\beta\gamma$  were found to follow the order syntaxin1A (EC<sub>50</sub> = 0.33  $\mu$ M), VAMP2 (0.94  $\mu$ M), and SNAP25 (1.07  $\mu$ M).

**Fig. 2 G $\beta\gamma$  interacts with the H3 domain of syntaxin1A and C-terminus of SNAP25.** (A) *Domain organization of syntaxin1A.* Fluorescent binding assays were performed with three variants of syntaxin1A: 1-266, which contains the Habc and H3 domains but lacks a

transmembrane region; 1-190, which contains the Habc domain and the Habc-H3 linker region; and 191-266, which contains the H3 domain. (B) *Quantification of the Gβγ/syntaxin1A interaction.* Syntaxin1A variants were cleaved from GST, and interaction with MIANS-Gβγ was detected by increased fluorescence output. The data represented ratio of RF at each different protein concentration. MIANS-Gβγ (20 nM) was found to interact with syntaxin1A (1-266) with an EC<sub>50</sub> of 0.33 μM and with the H3 domain syntaxin1A (191-266) with an EC<sub>50</sub> of 0.89 μM, while no significant interaction with syntaxin1A (1-190) was observed. (C) *Domain organization of SNAP25.* SNAP25 contains two SNARE motifs (SN1 and SN2). The C-terminus is cleaved specifically by two botulinum toxins, BoNT/E (between amino acids 180 and 181) and BoNT/A (196 and 197). (D) *Removal of the C-terminus of SNAP25 reduces affinity for Gβγ.* SNAP25 truncation mutants mimicking cleavage by BoNT/A (SNAP25Δ9) or BoNT/E (SNAP25Δ26) were tested for affinity for Gβγ using the fluorescent binding assay. MIANS-Gβγ (20 nM) was found to interact with SNAP25 with an EC<sub>50</sub> of 1.07 μM and with SNAP25Δ9 (mimics BoNT/A cleavage) with an EC<sub>50</sub> of 1.83 μM while no significant interaction with SNAP25Δ26 (mimics BoNT/E cleavage).

**Fig. 3 Gβγ-mediated inhibition of the synaptotagmin/SNARE interaction is diminished at high Ca<sup>2+</sup>-concentrations.** (A) *Preincubation with synaptotagmin (SytI) abrogates binding of Gβγ to the binary t-SNARE complex, indicating competition.* Binary t-SNARE complexes were assembled with syntaxin1A and SNAP25 in a 1:1 ratio, as shown by SDS-PAGE/Coomassie staining analysis (*inset*). Binding of 1 μM binary t-SNARE to 20 nM MIANS-Gβγ with (+ synaptotagmin) or without (- synaptotagmin) 250 nM synaptotagmin was measured by fluorescence enhancement in 50 μM Ca<sup>2+</sup>. (B) *Competition for binary t-SNARE binding is dose-*

*dependent.* The G $\beta\gamma$ /t-SNARE interaction was monitored as described in (A), and binding in the absence of synaptotagmin was normalized to 100%. % of RF is plotted against synaptotagmin protein concentration in 50  $\mu$ M Ca<sup>2+</sup>. (C) *Competition for binary t-SNARE binding is dependent on [Ca<sup>2+</sup>].* Different concentration of Ca<sup>2+</sup> (0-100  $\mu$ M) as noted was applied and % of RF was monitored (D) *Synaptotagmin and G $\beta\gamma$  compete for binding to the ternary SNARE complex.* In vitro reassembled ternary SNARE complex showed an SDS- and heat-stable species (*inset, lane 1*) that dissociated by additional heat treatment (*inset, lane 2*). Binding of the ternary SNARE complex with MIANS-G $\beta\gamma$  with or without 250 nM synaptotagmin was performed as described for Figure 3A. (E) *Competition for ternary SNARE binding is dependent on the concentration of synaptotagmin.* (F) *Competition for ternary SNARE binding is dependent on [Ca<sup>2+</sup>].* Panels A and D depict typical results from at least three experiments. Data are represented as mean  $\pm$  SEM (n=3).

**Fig. 4 G $\beta\gamma$  and synaptotagmin compete for binding to SNAP25 and syntaxin1A but not to VAMP2.** (A) *G $\beta\gamma$  competes with synaptotagmin for binding to syntaxin1A.* Competition assays were performed as described for Fig.3. The relative change in fluorescence of 20 nM MIANS-G $\beta\gamma$  in 100  $\mu$ M Ca<sup>2+</sup> upon addition of 0.5  $\mu$ M syntaxin1A was normalized to 100%. Addition of 20 nM synaptotagmin in the absence of Ca<sup>2+</sup> induced a slight decrease in the G $\beta\gamma$ /syntaxin1A interaction, but inclusion of both 20 nM synaptotagmin and 100  $\mu$ M Ca<sup>2+</sup> reduced binding by approximately 50%. (B) *G $\beta\gamma$  competes with synaptotagmin for binding to SNAP25.* 20 nM synaptotagmin caused a slight decrease in the interaction of 20 nM MIANS-G $\beta\gamma$  with 2  $\mu$ M SNAP25 in the absence of Ca<sup>2+</sup>, while inclusion of both 20 nM synaptotagmin and 100  $\mu$ M Ca<sup>2+</sup> reduced binding by approximately 80%. (C) *G $\beta\gamma$  and synaptotagmin do not compete for binding*

to VAMP2. The change in MIANS-G $\beta\gamma$  fluorescence upon addition of 2  $\mu\text{M}$  VAMP2, normalized to 100%, was not reduced significantly in the presence of 20 nM synaptotagmin, with or without 100  $\mu\text{M}$  Ca $^{2+}$ . Data are presented as mean  $\pm$  SEM (n = 3).

**Fig. 5 The C-terminal nine amino acids of SNAP25 comprise a critical region for competition between G $\beta\gamma$  and synaptotagmin.** G $\beta\gamma$  competition with synaptotagmin to bind ternary SNARE complex made up of SNAP25 (black bar) or SNAP25 $\Delta$ 9 (grey bar). G $\beta\gamma$  and SNARE complex binding was normalized to 100% fluorescence in the presence of 1 mM Ca $^{2+}$  and in the absence of synaptotagmin. Competition by synaptotagmin for G $\beta\gamma$  binding to SNARE containing SNAP25 $\Delta$ 9 was increased compared to the wild type SNARE complex (A) *Competition for binding to SNARE (SNAP25 $\Delta$ 9) is more sensitive to [Ca $^{2+}$ ].* (B) *Synaptotagmin I competes in a dose dependent manner with G $\beta\gamma$  for binding to SNARE, more potently with SNAP25 $\Delta$ 9.* Data are represented as mean  $\pm$  SEM (n=3).

**Fig. 6 Raising extracellular [Ca $^{2+}$ ] increases intracellular [Ca $^{2+}$ ] transients in a presynaptic terminal.** (A) *Lamprey giant axons labeled retrogradely with a Ca $^{2+}$ -sensitive dye (Fluo-4 dextran high affinity) and imaged with confocal microscopy. To quantify rapid action potential-induced Ca $^{2+}$  transients, high-speed line scanning of Ca $^{2+}$  entry (500 Hz) was repeated at the edge of the axon marked with the arrowheads.* (B - F) *Raising extracellular [Ca $^{2+}$ ] enhances action-potential-induced Ca $^{2+}$  influx.* (B) A single action potential in the axon evoked at the time point marked by the arrowhead caused a localized Ca $^{2+}$  transient in the axon. The line scan is pseudocolored with the lookup table shown below panel (A). The color values were measured and after background substraction, images were normalized to the baseline level of fluorescence

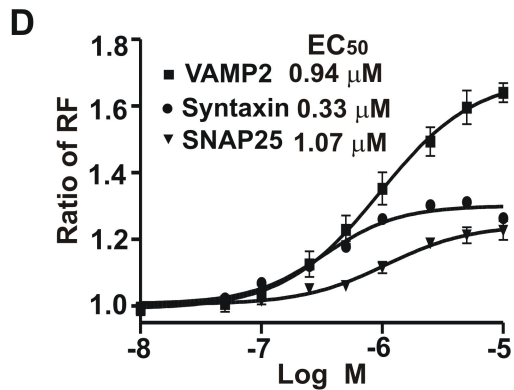
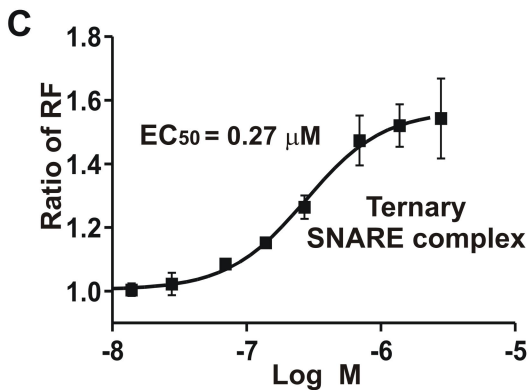
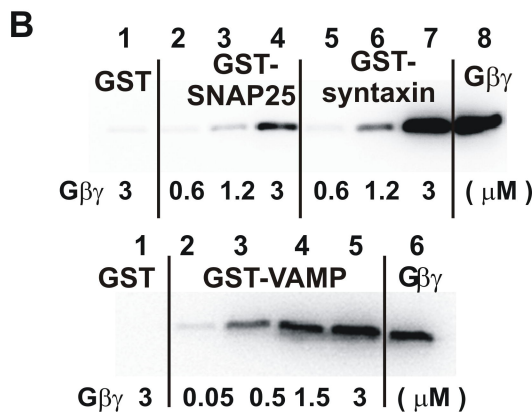
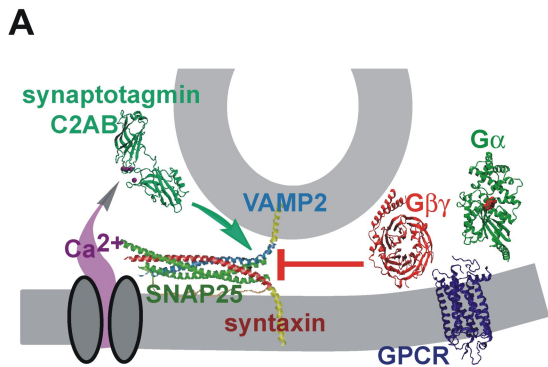
{DF/(F+1)}. (C) Increasing the extracellular  $\text{Ca}^{2+}$  concentration from 2.6 to 50 mM markedly enhanced the amplitude of the  $\text{Ca}^{2+}$  transient. (D) During wash-in of 50 mM  $\text{Ca}^{2+}$  the resting fluorescence was monitored at 30 s intervals. A small increase in the resting fluorescence was observed. Fluorescence is recorded to the same scale as (E). (E) The  $\text{Ca}^{2+}$  transients were measured between the white horizontal lines in (B) and (C) to quantify  $\text{Ca}^{2+}$  entry. Estimates of recorded  $\text{Ca}^{2+}$  transient amplitudes were made as described in methods. The calculated  $\text{Ca}^{2+}$  concentration scale for this estimate is shown to the right. (F) The relative effect of raising extracellular  $\text{Ca}^{2+}$  concentration on the amplitude of the axonal  $\text{Ca}^{2+}$  transient is recorded. Note that high extracellular  $\text{Ca}^{2+}$  concentrations have a proportionately smaller effect on the amplitudes of the recorded intracellular transient.

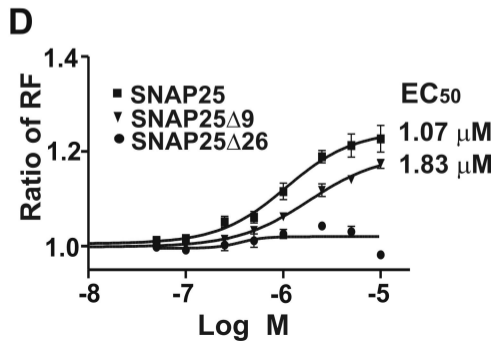
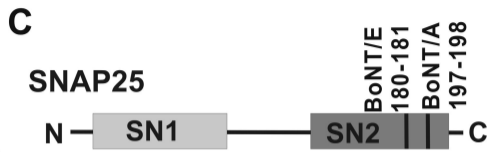
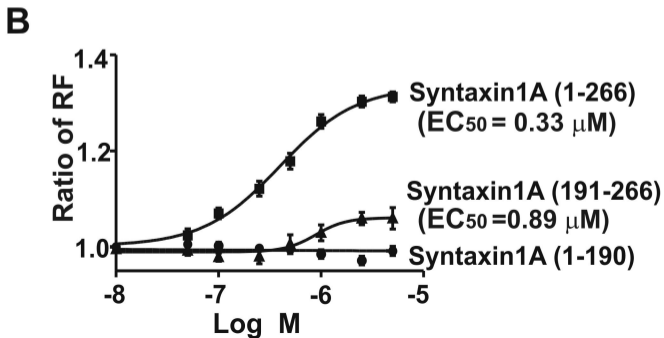
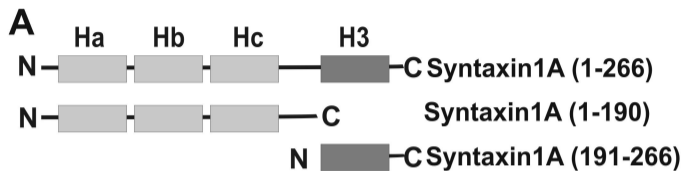
**Fig. 7 Raising extracellular  $[\text{Ca}^{2+}]$  decreases 5-HT-mediated inhibition of exocytosis in a presynaptic terminal.** (A) Increasing extracellular  $[\text{Ca}^{2+}]$  and, therefore the intracellular  $[\text{Ca}^{2+}]$  transients abrogates 5-HT-mediated inhibition of exocytosis. In a paired recording of presynaptic action potentials (upward peaks) and EPSCs (downward current peaks), a moderate dose of 5-HT (0.6  $\mu\text{M}$ ) applied in normal extracellular  $[\text{Ca}^{2+}]$  (2.6 mM) caused inhibition of exocytosis (blue). The EPSC recovered following 5-HT washout (top). The effect of 0.6  $\mu\text{M}$  5-HT is completely abrogated in 50 mM extracellular  $[\text{Ca}^{2+}]$  (red, bottom). (B) Pooled data shows the 5-HT-mediated inhibition in 2.6 mM and 50 mM  $\text{Ca}^{2+}$  ( $n=4-5$ , \*\*,  $P < 0.01$ ; \*,  $P < 0.05$ ). In control extracellular  $\text{Ca}^{2+}$  concentration, 0.6  $\mu\text{M}$  and 10  $\mu\text{M}$  of 5-HT significantly reduced the amplitude (blue). In 50 mM extracellular  $\text{Ca}^{2+}$ , 0.6  $\mu\text{M}$  5-HT no longer inhibited synaptic release and a saturating dose of 10  $\mu\text{M}$  of 5-HT slightly decreased the amplitude but was not statistically

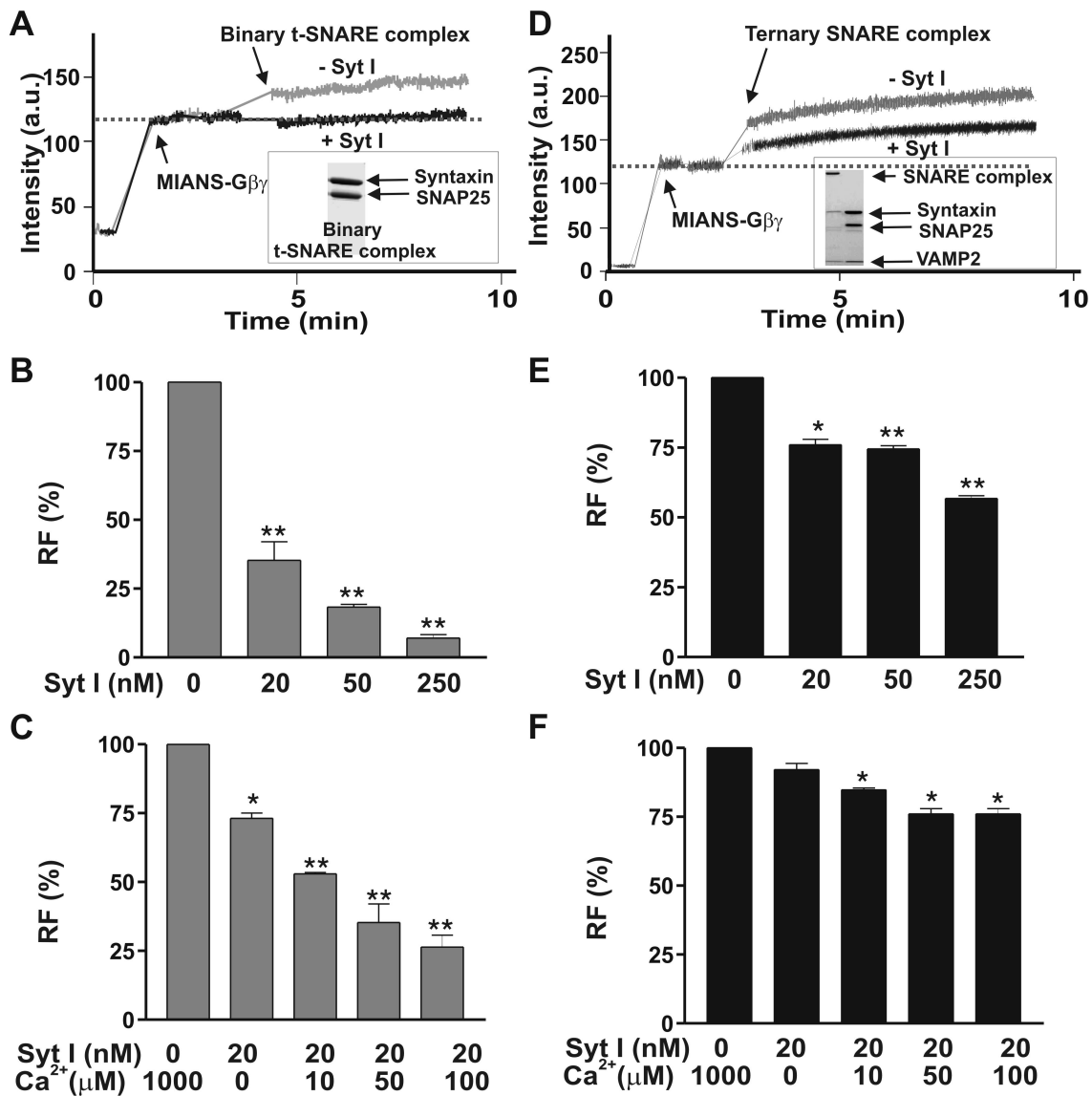


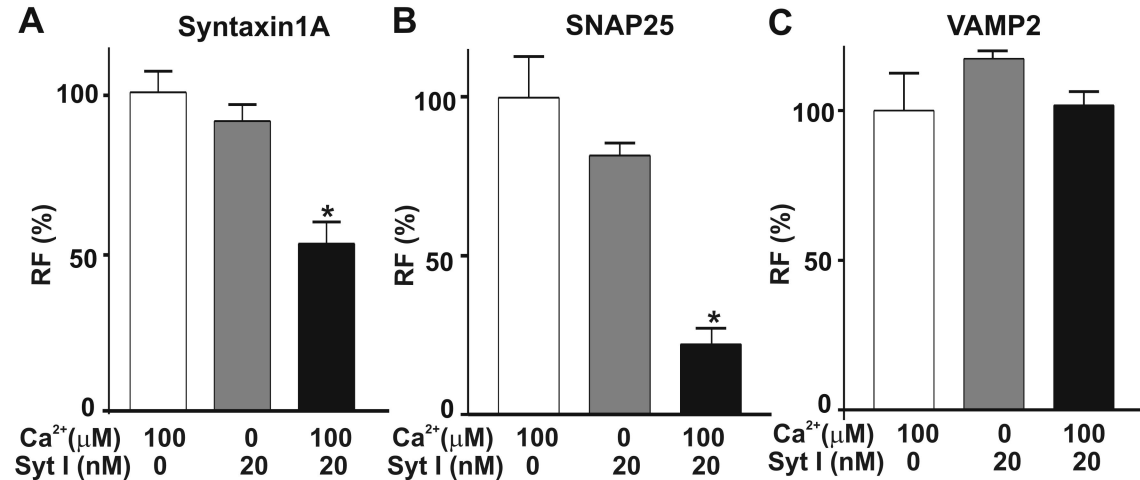
significant (red). (C) A comparison of the ability of moderate (0.6  $\mu\text{M}$ ) or high (10  $\mu\text{M}$ ) doses of 5-HT to inhibit exocytosis reveals that the level of exocytotic inhibition is highly dependent on the levels of both G protein activation and intracellular  $\text{Ca}^{2+}$ . The relative level of intracellular  $\text{Ca}^{2+}$  is indicated on the x-axis, while the degree of inhibition of exocytosis was measured as the EPSC response relative to control (no 5-HT) (y-axis).

**Fig. 8 High extracellular  $\text{Ca}^{2+}$  blocks the presynaptic inhibitory effect of  $\text{G}\beta\gamma$ .** (A) Increased extracellular  $[\text{Ca}^{2+}]$  causes a slight increase in exocytosis. A paired cell recording (top, presynaptic action potentials; bottom, resultant EPSCs) demonstrates the effect of raising extracellular  $\text{Ca}^{2+}$  from 2.6 mM (black trace) to 10 mM (grey). (B) The effect of presynaptic  $\text{G}\beta\gamma$  injection is reversed by raising the extracellular  $\text{Ca}^{2+}$  concentration. The responses observed in (A) were inhibited by injection of  $\text{G}\beta\gamma$  (blue). Subsequently raising the extracellular  $\text{Ca}^{2+}$  concentration reversed this inhibition (red). (C) Pooled data showing the effect of raising extracellular  $[\text{Ca}^{2+}]$  on the control synaptic responses and on the response in 10 mM  $\text{Ca}^{2+}$ . 10 mM extracellular  $\text{Ca}^{2+}$  enhanced the control response to  $122 \pm 2\%$  of control (n=3) (grey bar). In a further 4 paired cell recordings presynaptic injection of  $\text{G}\beta\gamma$  inhibited control responses to  $37 \pm 12\%$  of control (blue). Raising the extracellular  $\text{Ca}^{2+}$  concentration to 10 mM caused a recovery to  $100 \pm 9\%$  of control (red).

**Fig. 1**

**Fig. 2**

**Fig. 3**

**Fig. 4**

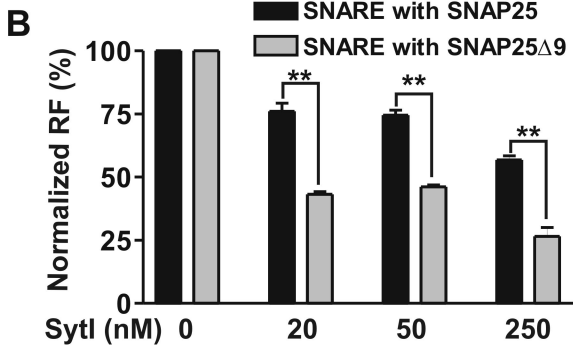
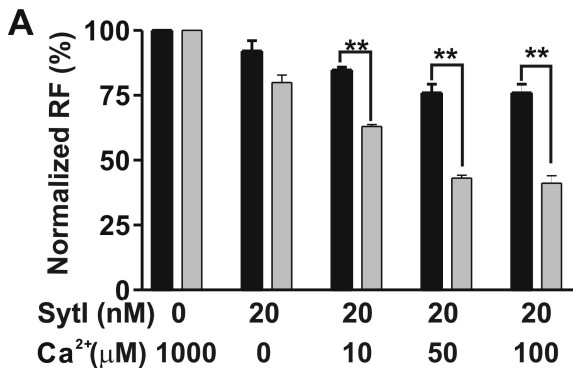
**Fig. 5**

Fig. 6

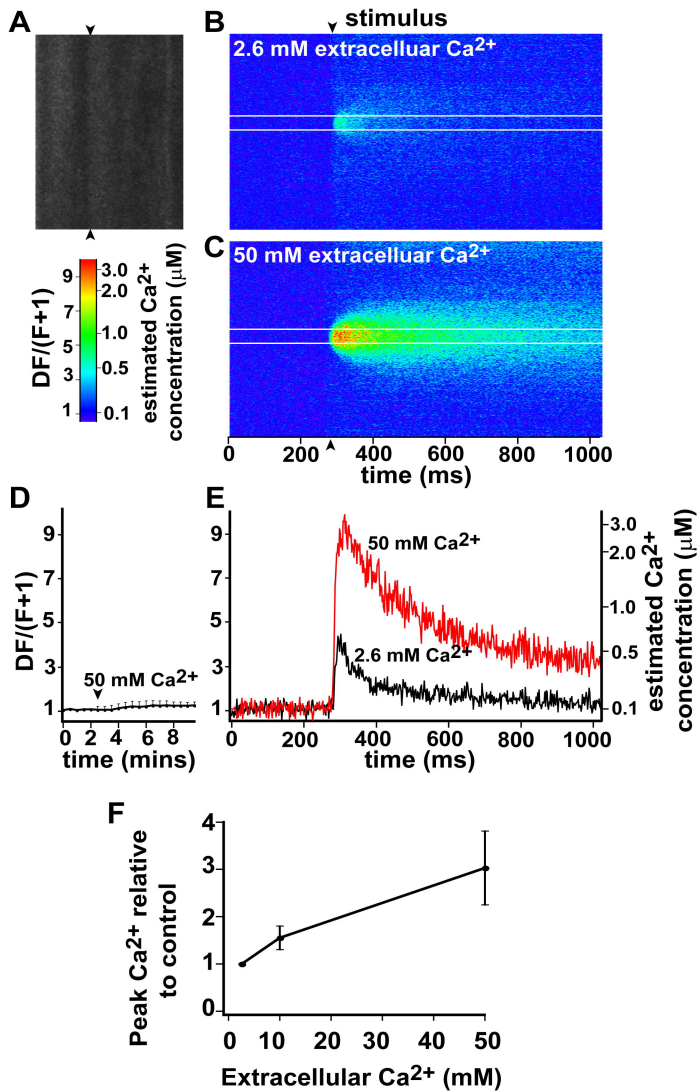


Fig. 7

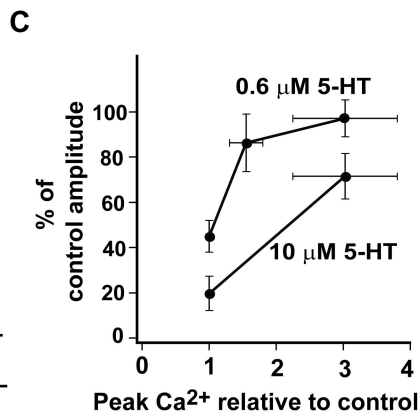
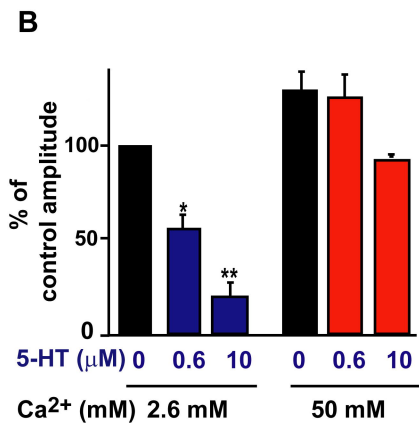
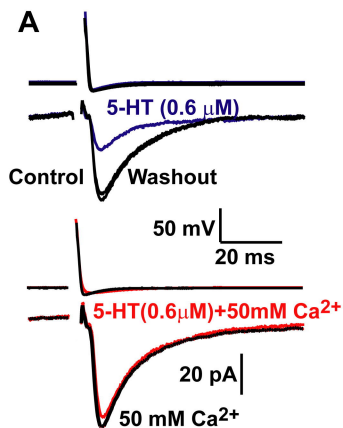




Fig. 8

